# Structure and Fluxional Behavior of *cis*-Bis(stannyl)bis(phosphine)platinum: Oxidative Addition of Organodistannane to Platinum(0) Complex

Yasushi Obora, Yasushi Tsuji,* Kayo Nishiyama,
Masahiro Ebihara, and Takashi Kawamura

*Department of Chemistry, Faculty of Engineering*
*Gifu University, Gifu 501-11, Japan*

*Received July 30, 1996*

Organodistannanes (**1**: $R_3Sn\text{-}SnR_3$) are useful reagents for double-stannylations of 1,3-dienes,[1a,b] alkynes,[1c] and allenes[1d] in the presence of a palladium-complex as a catalyst. In the catalytic cycle, oxidative addition of the Sn−Sn $\sigma$-bonds is believed to be a crucial step. However, there are only two precedents for it, and the resulting bis(stannyl) complexes have not been fully characterized. Clark and his co-worker described the first example of the oxidative addition of organodistannane (**1a**: $Me_3SnSnMe_3$) to $Pt(CH_2{=}CH_2)(PPh_3)_2$ or $Pt(PPh_3)_4$,[2a] but their reported geometry of the adduct is not consistent with our present study (*vide infra*). The second is the oxidative addition of the Sn−Sn bond of $Ph_2P(CH_2)_nMe_2SnSnMe_2(CH_2)_nPPh_2$ ($n$ = 2, 3) to $Pt(PPh_3)_4$ to afford a mixture of *cis*- and *trans*-isomers.[2b]

In this communication, we report structure and fluxional behavior of *cis*-bis(stannyl)bis(phosphine)platinum complexes, which were obtained by the oxidative addition of **1a** to platinum(0) phosphine complexes (**2**). The products have a distorted square-planar structure and show unique fluxional behavior. These features were investigated by multinuclear (including solid state $^{31}P$) NMR, X-ray crystallographic analysis, and *ab initio* molecular orbital calculation.

Hexamethyldistannane (**1a**) reacts with tetrakis[tri(4-methylphenyl)phosphine]platinum (**2a**) at −30 °C to afford the oxidative addition product (**3a**) (eq 1). The molecular structure of **3a** was determined by X-ray crystallographic analysis[3] as shown in Figure 1. The complex has a twisted square-planar structure with *cis*-orientation of the ligands. The structure is distinctly distorted from planarity: the dihedral angle between the $PtP_2$ and the $PtSn_2$ planes is 34.6°.

$$\mathrm{Me_3SnSnMe_3} \quad + \quad \mathrm{Pt(PR_3)_4} \longrightarrow \mathrm{Pt(SnMe_3)_2(PR_3)_2} \qquad (1)$$

| 1a | $R_3$ = | | $R_3$= | |
|---|---|---|---|---|
| | **2a**: $(4\text{-}MeC_6H_4)_3$ | | **3a**: $(4\text{-}MeC_6H_4)_3$ | 83% |
| | **b**: $(C_6H_5)_3$ | | **b**: $(C_6H_5)_3$ | 91% |
| | **c**: $(C_6H_5)_2Me$ | | **c**: $(C_6H_5)_2Me$ | 70% |

The solution $^{31}P$ NMR spectrum of **3a** at −90 °C (Figure 2a) showed resonances centered at 32.2 ppm with satellite peaks due to $^1J_{P-Pt}$ (2645 Hz, not shown in the Figure), $^2J_{P-Sn(transoid)}$ (1439 Hz with $^{117}Sn$ and 1507 Hz with $^{119}Sn$),[4] $^2J_{P-Sn(cisoid)}$ (181 Hz; peaks due to $^{117}Sn$ and $^{119}Sn$ were not resolved), and $^2J_{P-P}$ (13 Hz); only a central part of the spectrum is shown in Figure 2 with omitting satellite peaks due to the $^1J_{P-Pt}$ coupling.

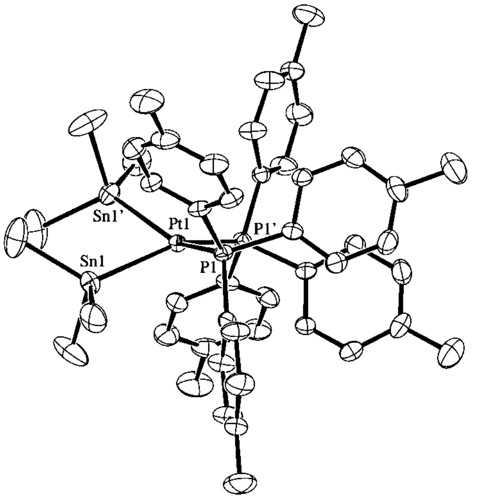

**Figure 1.** Molecular structure of **3a**. Hydrogen atoms are omitted for clarity. The Pt atom is on a crystallographic 2-fold axis. Selected bond distances (Å) and angles (deg): Pt1−Sn1 2.6289(6), Pt1−P1 2.299(1), Sn1−Pt1−Sn1′ 82.91(2), P1−Pt1−P1 104.23(6).

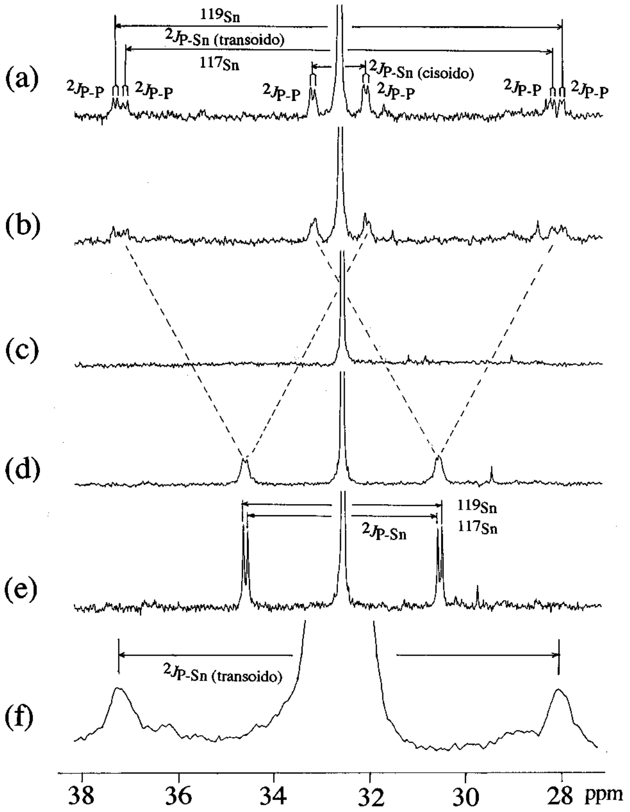

**Figure 2.** Central part of $^{31}P$ NMR spectra of **3a** (161.70 MHz). Solution NMR spectra measured in $CD_2Cl_2$ at (a) −90 °C, (b) −80 °C, (c) −50 °C, (d) −10 °C, (e) 20 °C, and (f) CPMAS solid-state NMR spectrum measured at room temperature. Chemical shifts are relative to $H_3PO_4$.

CPMAS solid-state $^{31}P$ NMR measured at room temperature (Figure 2f) shows the similar $^2J_{P-Sn(transoid)}$ (1500 Hz) and $^1J_{P-Pt}$ (2700 Hz, not shown in the figure) values, although $^2J_{P-Sn(cisoid)}$ coupling which is estimated to be ca. 180 Hz seems to be buried in the line width (300 Hz) of the main peak. The solution NMR spectra indicate that the complex shows reversible fluxional behavior. On warming, satellite peaks due to the two kinds of $^2J_{P-Sn}$ coalesced at −50 °C (Figure 2c) with maintaining the $^1J_{P-Pt}$ coupling (2644 Hz, not shown) and then sharpened at 20 °C with the averaged $^2J_{P-Sn}$ (629 Hz with $^{117}Sn$ and 663 Hz

---

(1) (a) Obora, Y.; Tsuji, Y.; Kakehi, T.; Kobayashi, M.; Shinkai, Y.; Ebihara, M.; Kawamura, T. *J. Chem. Soc., Perkin Trans. 1* **1995**, 599. (b) Tsuji, Y.; Kakehi, T. *J. Chem. Soc., Chem. Commun.* **1992**, 1000. (c) Piers, E.; Skerlj, R. T. *J. Org. Chem.* **1987**, *52*, 4421. (d) Mitchell, T. N.; Schneider, U. *J. Organomet. Chem.* **1991**, *407*, 319.

(2) (a) Akhtar, M.; Clark, H. C. *J. Organomet. Chem.* **1970**, *22*, 233. (b) Weichmann, H. *J. Organomet. Chem.* **1982**, *238*, C49.

(3) Crystal data of **3a**. Monoclinic, space group *C*2/*c*, yellow, $a$ = 19.369(7) Å, $b$ = 13.645(5) Å, $c$ = 18.056(3) Å, $\beta$ = 98.83(2)°, $V$ = 4715(2) Å$^3$, $Z$ = 4, $T$ = −136 °C, $d_{calcd}$ = 1.594 g cm$^{-3}$, $\mu$(Mo K$_\alpha$) = 40.96 cm$^{-1}$, $R$ = 0.029, $R_w$ = 0.027, GOF = 1.730.

(4) The ratio of the coupling constants coincides with that of the gyromagnetic ratio[4a] of $^{117}Sn$ and $^{119}Sn$, *viz.*, 0.956. (a) Brevard, C.; Granger, P. *Handbook of High Resolution Multinuclear NMR*; John Wiley & Sons: New York, 1981; p 168.

S0002-7863(96)02639-X CCC: $12.00

**Table 1.** $^{31}$P, $^{119}$Sn, and $^{195}$Pt NMR Data of **3a**−**c**[a]

| | **3a** | **3b** | **3c** *c*-**3c** | **3c** *t*-**3c** |
|---|---|---|---|---|
| $^{31}$P | 32.17 ppm | 32.28 ppm | 9.78 ppm | 11.00 ppm |
| $^{1}J_{P-Pt}$ | 2629 Hz | 2618 Hz | 2417 Hz | 2745 Hz |
| $^{2}J_{P-117Sn}$ | 629 Hz | 625 Hz | 653 Hz[b] | 169 Hz |
| $^{2}J_{P-119Sn}$ | 663 Hz | 653 Hz | 687 Hz[b] | 176 Hz |
| $^{119}$Sn | −15.24 ppm | −12.54 ppm | −29.90 ppm | 12.50 ppm |
| $^{1}J_{Sn-Pt}$ | 8559 Hz | 8532 Hz | 8389 Hz | 7269 Hz |
| $^{2}J_{Sn-P}$ | 663 Hz | 653 Hz | 687 Hz | 176 Hz |
| $^{195}$Pt | −5252 ppm | −5218 ppm | −5247 ppm | −5307 ppm |
| $^{1}J_{Pt-P}$ | 2629 Hz | 2618 Hz | 2417 Hz | 2745 Hz |

[a] $^{31}$P: 161.70 MHz, $^{119}$Sn: 148.95 MHz, $^{195}$Pt: 85.32 MHz. Chemical shifts are from $H_3PO_4$, $Me_4Sn$, and $H_2PtCl_6$, respectively. The spectra were measured at room temperature in $CD_2Cl_2$ (**3a** and **3b**) and in $C_6D_5CD_3$ (**3c**). [b] Measured at 70 °C.

with $^{119}$Sn)[4,5] (Figure 2e). The thermodynamic parameters were obtained by analyzing the line width alternation: $\Delta H^{\ddagger} = 42 \pm 1$ kJ mol$^{-1}$ and $\Delta S^{\ddagger} = 7.6 \pm 5.8$ J mol$^{-1}$ K$^{-1}$. The rate of the fluxional process depended on neither concentration of **3a** (from 8.8 mol dm$^{-3}$ to 22 mol dm$^{-3}$) nor the solvent employed, $CD_2Cl_2$ or $C_6D_5CD_3$. Furthermore, 1 molar excess of $P(4\text{-}MeC_6H_4)_3$ added to **3a** did not affect the rate.

Other platinum(0) phosphine complexes (**2b** and **2c**) also react with **1a** to afford the oxidative addition products (**3b** and **3c**) (eq 1). Although **3a** and **3b** consists of a single isomer, **3c** is a mixture of two isomers (*c*- and *t*-**3c** in 9:1 ratio). All the products including even **3c** showed good elementary analysis data. $^{31}$P, $^{119}$Sn, and $^{195}$Pt NMR spectral data of **3a**, **3b**,[6] and **3c** measured at room temperature are listed in Table 1. The $^{2}J_{P-Sn}$ values of **3a**, **3b**, and *c*-**3c** are similar (625−687 Hz), but that of *t*-**3c** is quite smaller (169 and 176 Hz). Importantly, *c*-**3c** showed analogous fluxional behavior ($\Delta H^{\ddagger} = 60 \pm 1$ kJ mol$^{-1}$ and $\Delta S^{\ddagger} = 32 \pm 5$ J mol$^{-1}$ K$^{-1}$), in which satellite peaks due to $^{2}J_{P-Sn}$ coalesced at 2 °C, and $^{2}J_{P-Sn(transoid)}$ (1482 Hz with $^{117}$Sn and 1551 Hz with $^{119}$Sn),[4] $^{2}J_{P-Sn(cisoid)}$ (177 Hz), and $^{2}J_{P-P}$ (21 Hz) appeared at −50 °C. These *J* values of *c*-**3c** are very close to those of **3a**. Accordingly, *c*-**3c** was assigned to *cis*-$[(Me_3Sn)_2(MePh_2P)_2Pt]$, while *t*-**3c** to the corresponding *trans*-isomer. The *trans*-isomer *t*-**3c** did not show any fluxional behavior at all. The ratio between *c*- and *t*-**3c** (9:1) did not change after 1 week at room temperature, indicating no interconversion between *c*- and *t*-**3c**.

The intramolecular conservation of the P and Sn nuclear spin states, which is shown by the sharp satellite peaks due to the $^{1}J_{P-Pt}$ and the line width alternation of the satellite peaks due to the $^{2}J_{P-Sn}$ in $^{31}$P NMR (Figure 2a−e), rules out dissociative mechanisms for the fluxional process. Associative processes are also unlikely, since the concentration of the complex, the coexistence of excess phosphine, and the nature of the solvent did not affect the fluxional process (*vide supra*). We attribute the fluxional process to the intramolecular twist-rotational motion *via* pseudo tetrahedral transition state (Scheme 1).[7]

*Ab initio* calculation[8] was carried out for $Pt(SnH_3)_2(PtH_3)_2$ as a model complex. The most stable calculated geometry (GS)

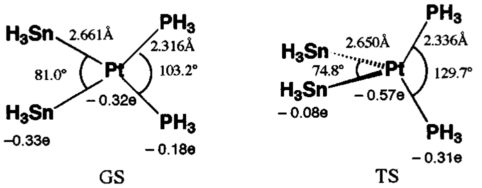

**Figure 3.** MP2-optimized geometries and Mulliken atomic charges on Pt, Sn, and P for ground (GS) and transition (TS) states.

**Scheme 1**

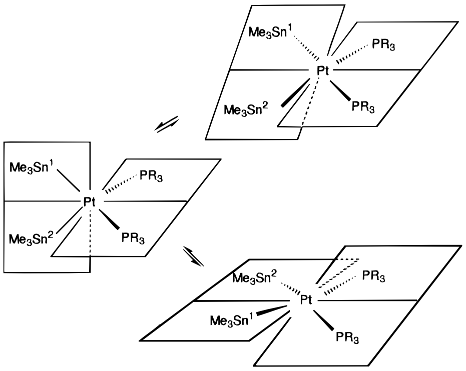

is planar (Figure 3). Thus, the distortion from planarity of **3a** may be attributed to steric effect associated with the substituents on the P and the Sn atoms. The activation energy of the fluxional process was calculated to be 80.0 kJ mol$^{-1}$, which is consistent with the experimental values. In the calculated transition state (TS), the P−Pt−P angle increases dramatically, and electron density was considerably transferred from the Sn onto the Pt and the P, suggesting decrease of the activation energy by introduction of electron withdrawing substituents on the P atoms and increase of it by substitution of the Sn with a more electronegative element such as C.

Addition of a chelate phosphine ($Ph_2P(CH_2)_nPPh_2$, $n = 2-4$) to a solution of **3a** displaced the $P(4\text{-}MeC_6H_4)_3$ completely, and the corresponding $Pt(SnMe_3)_2[Ph_2P(CH_2)_nPPh_2]$ (**3d**: $n = 2$, **3e**: $n = 3$, and **3f**: $n = 4$) was obtained quantitatively ($^{31}$P NMR). In contrast to the $^{31}$P NMR spectra of **3a**−**c**, those of **3d**−**f** showed $^{2}J_{P-Sn(transoid)}$ and $^{2}J_{P-Sn(cisoid)}$ couplings separately even at room temperature (see Supporting Information). The rotational motion of **3d**−**f** is slow on the NMR time scale; the satellite peaks due to the $^{2}J_{P-Sn(transoid)}$ and $^{2}J_{P-Sn(cisoid)}$ coalesced at 80 °C for **3d** and **3e** and at 50 °C for **3f**. With these chelate phosphines, the large P−Pt−P angle at the transition state, which would facilitate the rotation as suggested by the *ab initio* calculation, would not be attained easily.

**Acknowledgment.** This work was supported by the Grants-in-Aid for Scientific Research on Priority Area of Reactive Organometallics from the Ministry of Education, Science and Culture, Japan.

**Supporting Information Available:** Analytical data of **3a**−**c**, $^{31}$P NMR data of **3d**−**f** at room temperature, details of *ab initio* calculation, tables of crystal data and refinement details, atomic coordinates, thermal parameters, bond distances, bond angles and torsion angles of **3a** (17 pages). See any current masthead page for ordering and Internet access instructions.

JA9626392

---

[5] The $^{2}J_{P-Sn}$ values observed at 20 °C are equal to $(|^{2}J_{P-Sn(transoid)}| - |^{2}J_{P-Sn(cisoid)}|)/2$. Sign of the $^{2}J_{P-Sn(transoid)}$ and $^{2}J_{P-Sn(cisoid)}$ should be opposite.

[6] Clark *et al.* proposed that **3b** has the *trans*-structure. However, **3b** should have the same structure as **3a**, the *cis*-structure, since the both complexes show essentially the same NMR spectral data.

[7] For $NiX_2(PR_3)_2$ (X = Cl, Br, I) complexes, structural interconversion between square planar (diamagnetic) and tetrahedral (paramagnetic) isomers was reported.[7a] (a) La Mar, G. N.; Sherman, E. O. *J. Chem. Soc., Chem. Commun.* **1969**, 809, and references cited therein.

[8] Gausian 94 package. For details, see Supporting Information.